



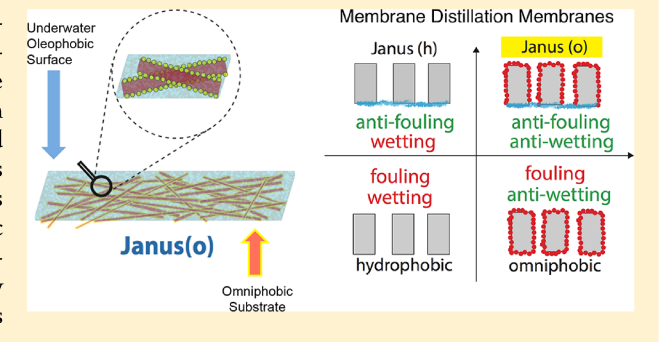
pubs.acs.org/est

Novel Janus Membrane for Membrane Distillation with Simultaneous Fouling and Wetting Resistance

Yu-Xi Huang,[†] Zhangxin Wang,[†] Jian Jin,[‡] and Shihong Lin*,^{†,}§

Supporting Information

ABSTRACT: A novel Janus membrane integrating an omniphobic substrate and an in-air hydrophilic, underwater superoleophobic skin layer was developed to enable membrane distillation (MD) to desalinate hypersaline brine with both hydrophobic foulants and amphiphilic wetting agents. Engineered to overcome the limitations of existing MD membranes, the Janus membrane has been shown to exhibit novel wetting properties unobserved in any existing membrane, including hydrophobic membranes, omniphobic membranes, and hydrophobic membranes with a hydrophilic surface coating. Being simultaneously resistant to both membrane fouling and wetting, a Janus membrane can sustain stable MD performance even with



challenging feed waters and can thus potentially transform MD to be a viable technology for desalinating hypersaline wastewater with complex compositions using low-grade-thermal energy.

■ INTRODUCTION

Membrane distillation (MD), a membrane based thermal distillation process capable of utilizing low-grade thermal energy to desalinate hypersaline brine water, 1-5 has been proposed as a promising candidate for treating reverse osmosis (RO) brine, highly saline industrial wastewater, and wastewater from unconventional energy production. 6-9 In an MD process, the transport of water vapor from the hot, saline solution (feed solution) to the cold distilled water (distillate) is driven by the temperature difference-induced partial vapor pressure difference across the membrane. ^{10,11} A typical MD membrane is hydrophobic and has micron-sized or submicron-sized pores (Figure 1A). This hydrophobic microporous structure of MD membranes serves two major roles in an MD process. First, the membrane prevents the direct liquid permeation of the salty feed solution through the pores and into the distillate, which is required for the MD process to have a high salt rejection (typically 99.9% or higher). This nonwetting condition demands hydrophobic materials to be used, as it is significantly more challenging for water to permeate through a hydrophobic pore than through a hydrophilic pore of the same size. The second function of the MD membrane is to provide a medium for efficient vapor transfer, which demands the membranes to have reasonably high porosity among other structural require-

The most typical membranes in existing MD studies were those made of polyvinylidene fluoride (PVDF), polypropylene (PP), and polytetrafluoroethylene (PTFE), which are common hydrophobic materials that can be readily processed into

microporous membranes. 12 MD membranes made of these materials function reasonably well with relatively "clean" feed waters such as seawater, RO brine, and industrial wastewater that contain mostly salt. However, when used to treat challenging feed waters, such as wastewater from industries and unconventional energy production sources, conventional hydrophobic materials fail for two major reasons: wetting and fouling. 13,14

The first major problem is membrane wetting facilitated by the presence of amphiphilic contaminants, such as surfactants, in the feedwater. These amphiphilic agents reduce the surface tension of the feedwater and thereby reduce the liquid entry pressure (LEP). Another possible mechanism for surfactants-induced wetting in MD is by rendering the membrane hydrophilic via surface adsorption of surfactants. The result of membrane wetting is the significantly reduced salt rejection due to the direct permeation of feed solution to the distillate (Figure 1B). The second major problem is membrane fouling by hydrophobic contaminants (foulants). 21-25 Because of the attractive hydrophobic interaction, hydrophobic foulants (e.g., oil droplets) tend to attach onto the hydrophobic membrane surface and possibly wick into the pores, thereby blocking the membrane pores and eliminating the medium for vapor transfer (Figure 1C).

June 5, 2017 Received: October 6, 2017 Revised: Accepted: October 30, 2017 Published: October 30, 2017

Department of Civil and Environmental Engineering, Vanderbilt University, Nashville, Tennessee 37235-1831, United States

[‡]Suzhou Institute of Nano-Tech and Nano-Bionics, Chinese Academy of Sciences, Suzhou 215123, P. R. China

Department of Chemical and Biomolecular Engineering, Vanderbilt University, Nashville, Tennessee 37235-1831, United States

Environmental Science & Technology

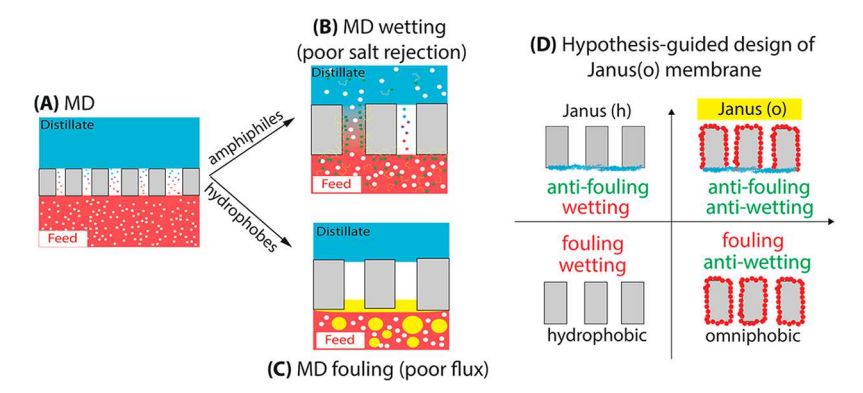


Figure 1. (A) Working mechanism of an MD process: driven by the temperature difference across the membrane, water evaporates at the feed/membrane interface, transports across the membrane pores as vapor, and condenses at the distillate/membrane interface. The white dots represent salts, which are rejected by the membrane. (B) Illustration of surfactant-induced wetting in an MD process: surfactants or amphiphilic contaminants reduce the surface tensions of the feedwater and/or render the MD membrane hydrophilic, thereby facilitating direct permeation of the feedwater through the pores. (C) Illustration of oil fouling in an MD process: oil droplets attach onto the membrane surface, coalesce, and block the pores for vapor transfer. (D) Illustration of the hypothesis that only a Janus membrane with an omniphobic substrate (i.e., a Janus(o) membrane) can achieve simultaneous fouling and wetting resistance.

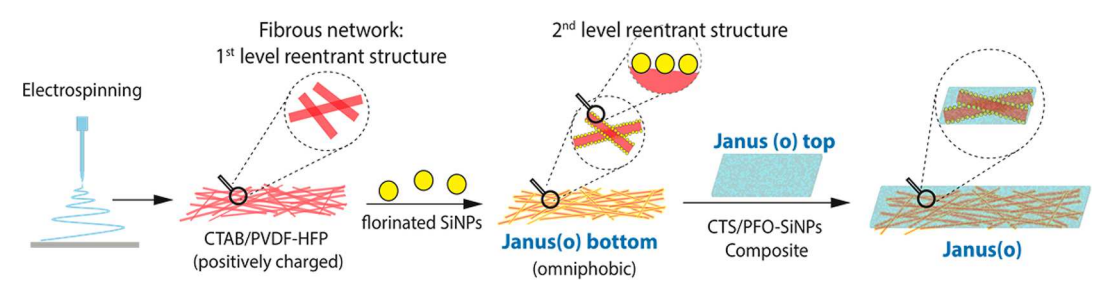


Figure 2. Fabrication procedure of the Janus(o) membrane. The first step involves electrospinning a fibrous substrate of CTAB/PVDF-HFP; the second step involves adsorption of SiNPs followed by surface fluorination; in the last step, a CTS/PFO-SiNPs nanoparticle—polymer composite coating was applied onto the omniphobic substrate.

In recent years, novel MD membranes with special wetting properties have been developed to overcome the problems of fouling and wetting in MD (Figure 1D). 13 Specifically, omniphobic membranes, membranes that are resistant to wetting by both oil and water droplets in air, have been developed to mitigate MD wetting induced by surfactants. It has been suggested that the reentrant structure that imparts the in-air omniphobicity is also responsible for maintaining the Cassie-Baxter state needed for wetting resistance of an omniphobic membrane. 16-18 On the other hand, it has been found that modifying a conventional hydrophobic MD membrane with an in-air hydrophilic surface coating, such as a hydrogel, can mitigate fouling by oil droplets in MD operations with oily feed solution. ^{23,26–28} The in-air hydrophilic coating is underwater oleophobic, deterring oil droplets from attaching to and spreading on the membrane surface and preventing them from blocking the pores of the underlying hydrophobic membrane.

However, there exists no membrane so far that can simultaneously resist wetting and fouling. An omniphobic membrane, which has shown to resist surfactant wetting, is actually underwater oleophilic. Oil droplets in feed readily fouled an omniphobic membrane and reduced water vapor flux by blocking the membrane pores. ¹³ On the other hand, a composite membrane with an in-air hydrophilic surface, which is fouling resistant, failed to mitigate membrane wetting by surfactants. Small amphiphilic molecules can readily penetrate the skin layer and impart a detrimental impact on the hydrophobic substrate. The development of a novel membrane

that is simultaneously resistant to wetting and fouling can enable MD to become universally applicable in desalinating hypersaline wastewater with complex compositions.

In this study, we develop a Janus membrane by integrating an omniphobic substrate and an in-air hydrophilic and underwater oelophobic skin layer. Hereafter, such a Janus membrane based on an omniphobic substrate will be called Janus(o) membrane, whereas a Janus membrane based on a hydrophobic substrate will be named Janus(h) membrane. Our central hypothesis is that, by integrating the unique functionalities of the two constituting layers, a Janus(o) membrane will outperform the Janus(h), omniphobic, and hydrophobic membranes in that only a Janus(o) membrane is resistant to both oil fouling and surfactant wetting (Figure 1D). We will prove this hypothesis by fabricating all these membranes and comparing their performances in MD fouling and wetting experiments.

MATERIALS AND METHODS

Materials and Chemicals. Poly(vinylidene fluoride-cohexafluoropropylene) (PVDF-HFP, $M_{\rm w}\approx 455\,000$), silica NPs (SiNPs, Ludox HS-40), fluorinated alkyl silane (FAS, 97%), sodium dodecyl sulfate (SDS, 99%), perfluorooctanoic acid, sodium hydroxide (NaOH), sodium chloride (NaCl), cetyltrimethylammonium bromide (CTAB, 98%), acetic acid (>99%), N,N-dimethylformamide (DMF, 99.8%), acetone (99.9%), and mineral oil were purchased from Sigma-Aldrich and used without purification. Chitosan (CTS, 90% Deacetylated) was obtained from Chemsavers (Bluefield, WV). Crude oil was acquired from Texas Raw Crude Oil (Midland, TX).

Design of the Janus(o) Membrane and Reference **Membranes.** To fabricate a Janus(o) membrane, we first create a positively charged electrospun fibrous substrate of CTAB/PVDF-HFP. The fibrous substrate was then decorated with fluorinated SiNPs, first by adsorption of negatively charged SiNPs onto the fibrous substrate using dip coating followed by fluorination using chemical vapor deposition. The resulting fibrous network is in-air omniphobic. Lastly, a layer of nanoparticle polymer composite made of SiNPs, chitosan (CTS), and perfluorooctanoate (PFO), SiNPs-CTS/PFO, was applied onto the omniphobic substrate using spray coating (Figure 2).

We also fabricated three other membranes listed in Figure 1D as the reference membranes for comparison in MD fouling and wetting experiments. The hydrophobic membrane was obtained by electrospinning a PVDF-HFP fibrous network. The Janus(h) membrane was fabricated by applying the SiNPs-CTS/PFO composite coating onto a hydrophobic PVDF-HFP membrane. The synthesis of the omniphobic membrane followed the exact same procedure as that for the Janus(o) membrane, but without the last step of applying the SiNPs-CTS/PFO composite surface coating.

Electrospinning of Fibrous Substrate. Two types of electrospun fibrous membrane substrates were prepared using electrospinning in this study. The first was the negatively charged PVDF-HFP substrate. This PVDF-HFP substrate was later used as a reference hydrophobic membrane and for fabricating the Janus(h) membrane. Both membranes were used as references in testing the performance of the Janus(o) membrane. The second type of electrospun fibrous substrate was made of CTAB impregnated PVDF-HFP (CTAB/PVDF-HFP). This CTAB/PVDF-HFP substrate was positively charged to facilitate the adsorption of SiNPs that were used to impart omniphobicity in the current study. The CTAB/ PVDF-HFP substrate was employed to fabricate the omniphobic membrane and the proposed Janus(o) membrane.

To prepare the dope solution for electrospinning, 2.8 g of PVDF-HFP was dissolved in a mixed solvent containing 9.8 g of DMF and 4.2 g of acetone. CTAB/PVDF-HFP solution was prepared by adding 50 mg of CTAB to the above PVDF-HFP solution. These solutions were stirred in a 45 °C water bath for 20 h. Electrospinning was conducted using a commercial electrospinning instrument with a rotating drum collector (TL-01, Tongli Tech., China), with the temperature maintained at 30 °C. For electrospinning of PVDF-HFP, 6 mL of PVDF-HFP solution was fed at 1.0 mL h⁻¹ using a syringe pump with an applied voltage of 10 kV. The electrospun fibrous scaffolds were collected onto an aluminum foil covering the grounded stainless drum with a rotating speed of 150 rpm. For electrospinning of CTAB/PVDF-HFP, the same parameters were used except that the applied voltage was 16 kV. When fabricating the Janus membrane, 5.5 mL of CTAB/PVDF-HFP was first electrospun, and then 0.5 mL of PVDF-HFP was spun on the surface of CTAB/PVDF-HFP. This two-layer substrate was created to facilitate the attachment of the hydrophilic coating layer onto the substrate, as coating adhesion onto the omniphobic substrate is significantly more challenging than onto a hydrophobic substrate. In all cases, the electrospun membranes have sufficient mechanical strength and maintained their integrity during all MD experiments.

SiNPs Adsorption and Surface Fluorination. The adsorption of SiNPs onto the CTAB/PVDF-HFP substrate was achieved using a dip-coating method. The CTAB/PVDF-

HFP substrate was first wetted by a 20% ethanol solution, followed by washing with deionized (DI) water to remove the ethanol. The wetted CTAB/PVDF-HFP substrate was then submerged into a suspension of 0.04% (mass to volume) SiNPs (pH 6.1) for 1 h. After dip-coating, the substrate was gently rinsed by DI water and dried in air. The fluorination of the SiNPs was achieved using chemical vapor deposition by exposing the SiNPs coated substrate to 0.15 mL of FAS in vacuum at 100 °C for 24 h.

CTS/PFO Composite Preparation and Coating. The CTS/PFO coating was prepared by dropwise addition of 0.1 M aqueous solution of perfluorooctanoate (PFO), obtained from the reaction of perfluorooctanonic acid with NaOH, into a dispersion of chitosan (CTS) and SiNPs mixture (0.2 g of CTS and 0.3 g of SiNPs in 100 mL of 1% acetic acid solution) under vigorous stirring. 22,29 After being rinsed with DI water and dried in air, 0.3 g of the prepared SiNPs-CTS/PFO coating was dispersed in 20 mL of ethanol using bath sonication to obtain the coating dispersion. This SiNPs-CTS/PFO antifouling skin layer was applied onto the electrospun substrate via spraying using an pressurized air-driven spray gun with an operation pressure of 0.2 MPa followed by heat treatment at 80 °C for 1 h. Such a coating layer was applied to the omniphobic substrate (with a thin PVDF-HFP skin layer) for fabricating the proposed Janus(o) membrane and to the PVDF-HFP substrate to prepare the Janus(h) membrane as reference for performance

Membrane Characterizations. Membrane morphology was characterized using scanning electron microscopy, or SEM (Zeiss Merlin). The ζ -potential was measured using a streaming potential analyzer (SurPASS, Anton Paar, Ashland, VA) with an adjustable gap cell. The surface wetting properties of top and bottom surfaces of the Janus(o) membrane were evaluated by measuring the in-air contact angle (CA) with several liquids (water, 4 mM SDS solution, mineral oil, and ethanol) and underwater CA with mineral oil, using an optical tensiometer (Theta Lite, Biolin Scientific). The underwater adhesion between oil and the membrane surfaces was assessed using oil probe force spectroscopy performed using a tensiometer (T114, Attension, Finland). The detailed procedure of the oil probe force spectroscopy was documented in our previous publications.²

MD Antiwetting and Antifouling Tests. We used direct contact MD configuration in all MD experiments for membrane performance testing, with feed and distillate temperatures maintained to be 60 and 20 °C, respectively. We constantly measured the cumulative mass and the conductivity of distillate, from which the real-time water flux and salt rejection were calculated. Detailed information about the MD cell and the system flowchart (Schematic S1) can be found in the Supporting Information (SI). The Janus(o) membrane was challenged in MD experiments with feed solutions containing either oil foulants or amphiphilic surfactants. Its MD performance, in terms of normalized flux and salt rejection, was compared to that of the reference membranes including the hydrophobic PVDF-HFP membrane, the omniphobic membrane, and the Janus(h) membrane.

The fouling experiments were conducted using an oily saline feed solution with 1,000 ppm (wt %) crude oil and a salinity of 35 g L⁻¹ (NaCl). This oily saline feed solution was prepared by mixing 2 g of crude oil with 2 L of NaCl aqueous solution at 16 000 rpm for 15 min using a homogenizer (Fisher Scientific, Waltham, MA). The resulting oil-in-water emulsion with

micron-sized oil droplets $(5.0 \pm 0.75 \,\mu\text{m})$ was kinetically stable with no observable phase separation overnight (Figure S1).

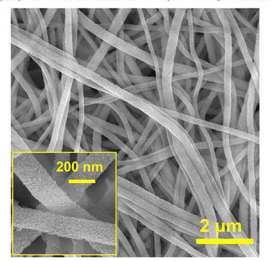
For MD wetting experiments, SDS was added as the amphiphilic agent to the feed solution for inducing membrane pore wetting. The addition of SDS was incremental so that the SDS concentrations of the feed solution after three additions were 0.1, 0.2, and 0.4 mM, respectively. The flow rates of feed and distillate streams were controlled to be 0.45 and 0.2 L min⁻¹, respectively, so that the feed hydraulic pressure was slightly higher than that of distillate stream with our MD setup. This operation condition facilities unambiguous detection of wetting if it occurs, as it certainly leads to increases in both water flux and distillate salinity. Both fouling and wetting experiments were performed in replicates with only one set of representative results presented in the following discussions.

■ RESULTS AND DISCUSSION

Morphology and Wetting Properties of the Janus(o) Membranes. The electrospun CTAB/PVDF-HFP substrate of the Janus(o) membrane has a fibrous structure with a mean fiber diameter of 188 ± 22 nm (Figure 3A). These fibers are

(A) Janus bottom (omniphobic)





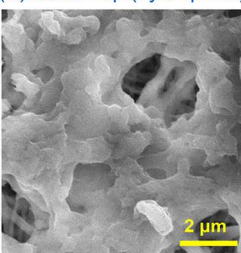


Figure 3. (A) SEM image of the Janus membrane substrate. The inset features the SiNPs on individual fibers. (B) SEM image of the SiNPs-CTS/PFO nanoparticle—polymer composite coating on a Janus membrane surface.

significantly smaller in diameter than the PVDF-HFP fibers without CTAB (Figure S2), possibly due to the higher charge density of the dope solution that led to more significant stretching under the strong electric field. Streaming potential measurements suggest that the CTAB/PVDF-HFP fibrous network is positively charged when pH is below 7, whereas the PVDF-HFP matrix is negatively charged throughout the pH range tested (Figure S3). The positive charges on the CTAB/PVDF-HFP fibers facilitated the adsorption of SiNPs. Nanoscale SiNPs were clearly observed on individual fibers (Figure

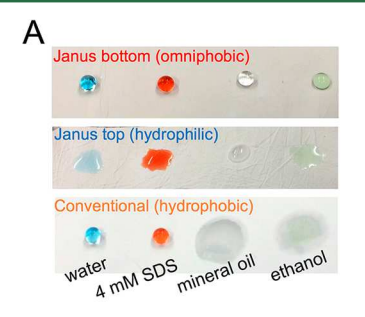
3A, inset) after dip-coating, yielding a second level reentrant structure on top of the first level reentrant structure imparted by the fibrous network itself.^{30–33} The skin layer of the Janus(o) membrane is composed of a SiNPs-CTS/PFO composite that formed a continuous and rough surface with micron-sized pores (Figure 3B).

The in-air contact of different liquids with the top and bottom surfaces of the Janus(o) membrane, and with surface of a hydrophobic PVDF-HFP membrane, is shown in Figure 4A. The in-air CAs with different liquids and the underwater CAs with mineral oil for the same three surfaces are summarized in Figure 4B. The in-air CAs of the PVDF-HFP membrane were $136.4 \pm 2.4^{\circ}$ and $127.4 \pm 2.7^{\circ}$ for water and 4 mM SDS solution, respectively. However, mineral oil ($\gamma \approx 30 \text{ mN m}^{-1}$) and ethanol ($\gamma = 22.1 \text{ mN m}^{-1}$)¹⁸ completely wicked the PVDF-HFP membrane. In contrast, the omniphobic bottom of the Janus(o) membrane was able to resist wetting by all tested liquids, yielding in-air CAs of $156.9 \pm 0.8^{\circ}$, $145.6 \pm 4.5^{\circ}$, 159.9 \pm 4.3°, and 95.4 \pm 1.4° for water, 4 mM SDS solution, mineral oil, and ethanol, respectively. None of the liquids, regardless of surface tension, was able to wick through the omniphobic substrate due to the presence of dual-scale reentrant architecture. The in-air CAs of the same tested liquids on the top surface of the Janus membrane were rather low (Figure 4B), suggesting the coated surface was in-air amphiphilic.

Comparing the wetting properties between the hydrophobic PVDF-HFP membrane and the in-air amphiphilic top surface of the Janus(o) membrane (Figure 4A), it was interesting to observe that while a conventional hydrophobic membrane was resistant to wetting by high-surface-tension liquids but wicked by low-surface-tension liquids, the top surface of a Janus(o) membrane was wetted by all but not wicked by any of the tested liquids. This special wetting property of the Janus(o) membrane results from the combination of an in-air amphiphilic skin layer that all liquids can wet and an omniphobic substrate that no liquid can penetrate through.

The surface wetting properties directly relevant to membrane fouling were elucidated by underwater—oil CAs measured with a mineral droplet on membrane samples inversely submerged in water. Both the reference hydrophobic membrane and the omniphobic bottom of the Janus(o) membrane exhibited very low underwater—oil CAs (Figure 4B), which was consequent of the strong attractive hydrophobic interaction between oil and the low-surface-energy materials of the hydrophobic or omniphobic fibrous network.

13,34—36 However, an omniphobic porous substrate, even without the hydrophilic SiNPs-CTS/PFO surface coating, differed significantly from the hydro-



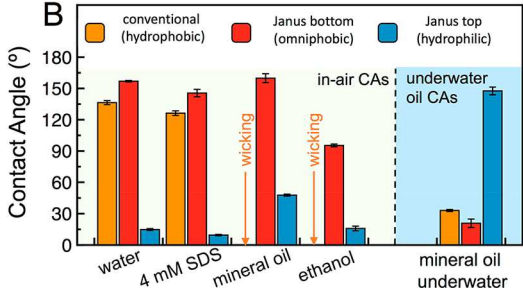


Figure 4. (A) Photographic images of different liquid droplets on the bottom surface and top surface of the Janus(o) membrane and on the hydrophobic PVDF-HFP membrane. (B) Left of the dashed line (yellow background): In-air sessile drop CAs for three different surfaces (in-air hydrophobic, omniphobic, and hydrophilic) with four liquids (water, 4 mM SDS solution, mineral oil, and ethanol). Right of the dashed line (blue background): underwater CAs for the three surfaces with mineral oil.

phobic membrane in that the oil droplet was able to wick through the hydrophobic membrane but not the omniphobic porous substrate, which was evidenced by the clearly observable oil stain on the back of the hydrophobic membrane but not on that of a standalone omniphobic membrane. Similar to mechanism behind its in-air omniphobicity, the ability of an standalone omniphobic fibrous network to resist wicking by a spreading oil puddle underwater is attributable to the Cassie-Baxter state sustained by both low-surface-energy material and hierarchical reentrant texture. 30,3

In comparison, the SiNPs-CTS/PFO coated surface of the Janus membrane was underwater superoleophobic (Figure 4B) due to the hydration of the rough nanoparticle—polymer composite coating layer.^{37–40} For the oil droplet to spread over and physically contact the Janus membrane surface, the hydration layer on the SiNPs-CTS/PFO surface has to be eliminated, which is thermodynamically highly unfavorable. 41-44 Moreover, the presence of SiNPs enhances the surface roughness and thus the hydration area, which further augments the hydration force and renders the surface underwater superoleophobic.²

Oil probe force spectroscopy was also conducted to assess the interaction between an oil droplet and surfaces with different wetting properties, which is strongly relevant to understanding the impact of surface wettability on membrane fouling propensity. The force curves on Figure 5 indicate strong

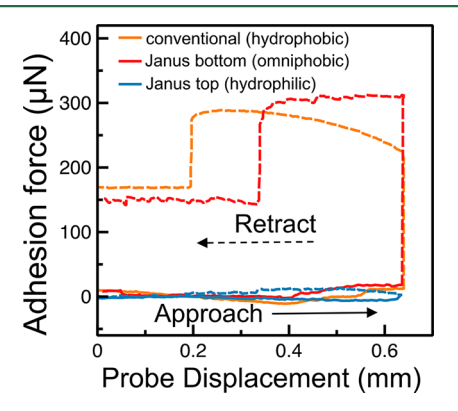


Figure 5. Force curves from tensiometer-based oil probe force spectroscopy for the hydrophobic, omniphobic (Janus bottom), and hydrophilic (Janus top) surfaces.

attraction of oil droplets to both a reference hydrophobic PVDF-HFP membrane and an omniphobic membrane (same as the substrate of a Janus(o) membrane) and significant retention of oil droplets by these two membranes. This implies that severe membrane fouling would likely occur with both hydrophobic and standalone omniphobic MD membranes if the MD feed solution contains hydrophobic contaminants. In comparison, no attractive oil-membrane interaction or oil retention by the surface was observed with the SiNPs-CTS/ PFO coated top surface of the Janus membrane. The qualitative comparison between interactions with different surfaces, which was consistent between multiple sets of force curve measurements, correlate well with the measured underwater-oil CAs.

Wetting Resistance of the Janus(o) Membrane. The Janus(o) membrane was challenged in MD experiments using feed solution with progressively increasing SDS concentration to evaluate its wetting resistance. For comparison, the same experiments were conducted using a hydrophobic PVDF-HFP membrane, a Janus(h) membrane, and an omniphobic

membrane. Figure 6A shows the time-dependent normalized fluxes and salt rejections for both the hydrophobic and

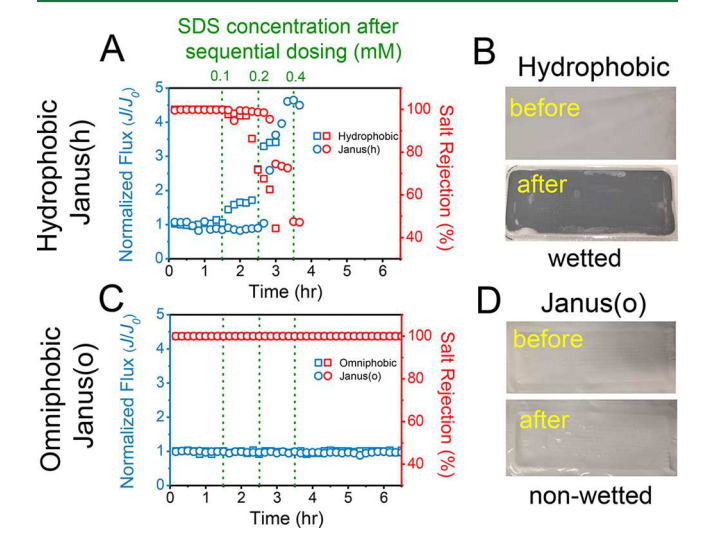


Figure 6. (A, C) Normalized water flux, J/J_0 , (blue) and salt rejection (red) for MD wetting experiments. (B, D) Photographic images of the membranes before and after the wetting experiments. For all MD experiments, the feed and distillate temperatures were 60 and 20 °C, respectively.

Janus(h) membranes. Both membranes were wetted in the presence of SDS, with the hydrophobic and Janus(h) membranes failing at SDS concentrations of 0.1 and 0.2 mM, respectively. Consequently, the water fluxes increased by multiple times, and the salt rejection significantly dropped (note that a salt rejection below 99% is considered unacceptable in MD). The wetting of the hydrophobic PVDF-HFP membrane can also be clearly observed by visually inspecting the membrane after the MD experiments: the feed solution wicked through the membrane pores completely, rendering the wetted membrane translucent (Figure 6B). As a result, the distillate became unacceptably saline due to the direct permeation of the saline feed solution through the wetted

In comparison, the Janus(o) membrane and the omniphobic membrane were able to sustain a stable MD performance even in the presence of 0.4 mM SDS, evidenced by the stable water vapor flux and perfect salt rejection. Visual inspection of the Janus(o) membrane before and after the experiment suggests that, although the top surface of the Janus(o) membrane was wetted due to its hydrophilicity, the feed solution was not able to wick through the underlying omniphobic substrate. The prevention of the penetration of feed solution with surfactants through the membrane pores was rendered possible by the hierarchical reentrant structure of the omniphobic fibrous network. 16-18,45

Fouling Resistance of the Janus(o) Membrane. In MD experiments with oil-in-water emulsion as the feed solution, the hydrophobic PVDF-HFP membrane and the omniphobic membrane were fouled rapidly, with their water vapor fluxes dropping to less than 20% of the initial flux within 1 h of operation, even though the salt rejection was unaffected (Figure 7A). Visual inspection of the PVDF-HFP membrane before and after the experiments also reveals that the membrane was severely fouled with oil stains on the surface (Figure 7B). Rinsing the membrane surface with DI water was not able to

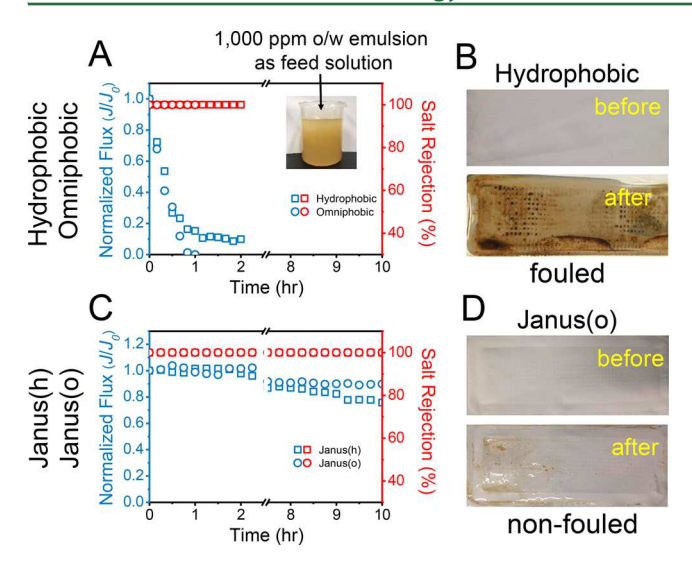


Figure 7. (A, C) Normalized water fluxes, J/J_0 , (blue) and salt rejections (red) for MD fouling experiments with the hydrophobic membrane (A) and the Janus membrane (C), respectively. (B, D) Photographic images of the membranes before and after the fouling experiments for the hydrophobic membrane (A) and the Janus membrane (C), respectively. For all MD experiments, the feed and distillate temperatures were 60 and 20 °C, respectively. The feed solution was a saline oil-in-water emulsion with 35 g/L NaCl and 1000 ppm crude oil. The initial water fluxes for hydrophobic, omniphobic, Janus(h), and Janus(o) were 34.1, 13.3, 24.7, and 14.1 L m-2 h-1 respectively. We have conducted additional MD experiments for the hydrophobic membrane with the feed and distillate temperatures being 60 and 30 °C, respectively. With this higher distillate temperature, the flux was reduced to 13.9 L m⁻² h⁻¹ (Figure S4), which was comparable to the fluxes of the omniphobic and Janus(o) membrane. This additional experiment was performed to demonstrate that fouling of the hydrophobic PVDF membrane was not due to its higher initial flux which, beyond a critical level, may strongly promote oil fouling.40

remove those stains, suggesting the irreversibility of fouling. The Janus membranes, including both Janus(o) and Janus(h) membranes, on the other hand, were able to sustain stable MD performance with both their fluxes and salt rejections remaining near constant over 10 h of operation (Figure 7C). The adhesion of oil foulants onto the Janus(o) membrane surface was minimal according to visual inspection of the Janus membrane after the fouling experiments (Figure 7D).

The MD performances of the hydrophobic and Janus membranes in the presence of oil foulants are well corroborated by the measured underwater-oil CAs and the results from the oil-probe force spectroscopy. The presence of the SiNPs-CTS/ PFO coating rendered the surface Janus membranes underwater superoleophobic and resistant to the adhesion of micronsized crude oil droplets. Because the crude oil droplets were significantly larger than the characteristic pore size of the SiNPs-CTS/PFO coating layer, the transport of oil droplets across this coating layer to reach the underlying hydrophobic or omniphobic substrates was both energetically and sterically impeded. Consequently, the hydrophobic oil droplets did not affect the underlying omniphobic substrate of the Janus membrane.

■ IMPLICATIONS

The recent developments in engineering materials with novel wetting properties have significantly advanced membrane-based separations, not only by enhancing the performance of existing

technologies but, more importantly, by enabling new technologies or existing technologies for new applications that were not feasible with conventional materials. This study showcases a perfect example of how engineering the surface wettability can enable an existing desalination process, MD, to treat challenging feedwater that it failed to treat. The Janus(o) membrane reported herein, with an antiwetting omniphobic substrate and an antifouling skin layer, empowers MD to desalinate hypersaline wastewater with amphiphilic and/or hydrophobic constituents.

ASSOCIATED CONTENT

S Supporting Information

The Supporting Information is available free of charge on the ACS Publications website at DOI: 10.1021/acs.est.7b02848.

Details on the MD experimental setup and conditions, microscopic image and size distribution of the oil-inwater emulsion, SEM image of PVDF-HFP/CTAB and its fiber diameter distribution, and ζ -potentials of the PVDF-HFP and PVDF-HFP/CTAB electrospun membranes. (PDF)

AUTHOR INFORMATION

Corresponding Author

*Phone: +1 (615) 322-7226; email: shihong.lin@vanderbilt.

ORCID

Jian Jin: 0000-0002-7279-2903 Shihong Lin: 0000-0001-9832-9127

The authors declare the following competing financial interest(s): A patent application has been filed based on the idea and findings reported in the submitted manuscript.

ACKNOWLEDGMENTS

We acknowledge the financial support from National Science Foundation via Grants CBET-1705048 and CBET-1739884.

REFERENCES

- (1) Banat, F.; Jwaied, N. Economic evaluation of desalination by small-scale autonomous solar-powered membrane distillation units. Desalination 2008, 220 (1-3), 566-573.
- (2) Al-Obaidani, S.; Curcio, E.; Macedonio, F.; Di Profio, G.; Al-Hinai, H.; Drioli, E. Potential of membrane distillation in seawater desalination: Thermal efficiency, sensitivity study and cost estimation. J. Membr. Sci. 2008, 323 (1), 85-98.
- (3) Kim, Y. D.; Thu, K.; Ghaffour, N.; Choon Ng, K. Performance investigation of a solar-assisted direct contact membrane distillation system. J. Membr. Sci. 2013, 427, 345-364.
- (4) Dow, N.; Gray, S.; Li, J. de; Zhang, J.; Ostarcevic, E.; Liubinas, A.; Atherton, P.; Roeszler, G.; Gibbs, A.; Duke, M. Pilot trial of membrane distillation driven by low grade waste heat: Membrane fouling and energy assessment. Desalination 2016, 391, 30-42.
- (5) Dudchenko, A. V.; Chen, C.; Cardenas, A.; Rolf, J.; Jassby, D. Frequency-dependent stability of CNT Joule heaters in ionizable media and desalination processes. Nat. Nanotechnol. 2017, 12, 557-
- (6) Shaffer, D. L.; Arias Chavez, L. H.; Ben-Sasson, M.; Romero-Vargas Castrillón, S.; Yip, N. Y.; Elimelech, M. Desalination and reuse of high-salinity shale gas produced water: drivers, technologies, and future directions. Environ. Sci. Technol. 2013, 47 (17), 9569-9583.
- (7) Camacho, L. M.; Dumée, L.; Zhang, J.; Li, J. De; Duke, M.; Gomez, J.; Gray, S. Advances in membrane distillation for water

- desalination and purification applications. Water (Basel, Switz.) 2013, 5
- (8) Duong, H. C.; Duke, M.; Gray, S.; Nelemans, B.; Nghiem, L. D. Membrane distillation and membrane electrolysis of coal seam gas reverse osmosis brine for clean water extraction and NaOH production. Desalination 2016, 397, 108-115.
- (9) Tong, T.; Elimelech, M. The Global Rise of Zero Liquid Discharge for Wastewater Management: Drivers, Technologies, and Future Directions. Environ. Sci. Technol. 2016, 50 (13), 6846-6855.
- (10) Lawson, K. W.; Lloyd, D. R. Membrane distillation. J. Membr. Sci. 1997, 124 (1), 1-25.
- (11) Khayet, M.; Matsuura, T. Membrane Distillation; Elsevier: Amsterdam, 2011.
- (12) Zhang, J.; Dow, N.; Duke, M.; Ostarcevic, E.; Li, J. D.; Gray, S. Identification of material and physical features of membrane distillation membranes for high performance desalination. J. Membr. Sci. 2010, 349 (1-2), 295-303.
- (13) Wang, Z.; Lin, S. Membrane fouling and wetting in membrane distillation and their mitigation by novel membranes with special wettability. Water Res. 2017, 112, 38-47.
- (14) Tijing, L. D.; Woo, Y. C.; Choi, J. S.; Lee, S.; Kim, S. H.; Shon, H. K. Fouling and its control in membrane distillation-A review. J. Membr. Sci. 2015, 475, 215-244.
- (15) Razmjou, A.; Arifin, E.; Dong, G.; Mansouri, J.; Chen, V. Superhydrophobic modification of TiO2 nanocomposite PVDF membranes for applications in membrane distillation. J. Membr. Sci. 2012, 415-416, 850-863.
- (16) Lin, S.; Nejati, S.; Boo, C.; Hu, Y.; Osuji, C. O.; Elimelech, M. Omniphobic Membrane for Robust Membrane Distillation. Environ. Sci. Technol. Lett. 2014, 1 (11), 443-447.
- (17) Boo, C.; Lee, J.; Elimelech, M. Engineering Surface Energy and Nanostructure of Microporous Films for Expanded Membrane Distillation Applications. Environ. Sci. Technol. 2016, 50 (15), 8112-
- (18) Lee, J.; Boo, C.; Ryu, W. H.; Taylor, A. D.; Elimelech, M. Development of Omniphobic Desalination Membranes Using a Charged Electrospun Nanofiber Scaffold. ACS Appl. Mater. Interfaces 2016, 8 (17), 11154-11161.
- (19) Boo, C.; Lee, J.; Elimelech, M. Omniphobic Polyvinylidene Fluoride (PVDF) Membrane for Desalination of Shale Gas Produced Water by Membrane Distillation. Environ. Sci. Technol. 2016, 50 (22), 12275-12282.
- (20) Liao, Y.; Loh, C. H.; Wang, R.; Fane, A. G. Electrospun superhydrophobic membranes with unique structures for membrane distillation. ACS Appl. Mater. Interfaces 2014, 6 (18), 16035-16048.
- (21) Gryta, M.; Tomaszewska, M.; Grzechulska, J.; Morawski, a. W. Membrane distillation of NaCl solution containing natural organic matter. J. Membr. Sci. 2001, 181 (2), 279-287.
- (22) Wang, Z.; Hou, D.; Lin, S. Composite Membrane with Underwater-Oleophobic Surface for Anti-Oil-Fouling Membrane Distillation. Environ. Sci. Technol. 2016, 50 (7), 3866-3874.
- (23) Zuo, G.; Wang, R. Novel membrane surface modification to enhance anti-oil fouling property for membrane distillation application. J. Membr. Sci. 2013, 447, 26-35.
- (24) Warsinger, D. M.; Swaminathan, J.; Guillen-Burrieza, E.; Arafat, H. A.; Lienhard V, J. H. Scaling and fouling in membrane distillation for desalination applications: A review. Desalination 2015, 356, 294-
- (25) Qin, W.; Zhang, J.; Xie, Z.; Ng, D.; Ye, Y.; Gray, S.; Xie, M. Synergistic effect of combined colloidal and organic fouling in membrane distillation: measurements and mechanisms. Environ. Sci. Water Res. Technol. 2017, 3, 119-127.
- (26) Wang, Z.; Elimelech, M.; Lin, S. Environmental applications of interfacial materials with special wettability. Environ. Sci. Technol. 2016, 50, 2132-2150.
- (27) Wang, Z.; Lin, S. The Impact of Low-surface-energy Functional Groups on Oil Fouling Resistance in Membrane Distillation. J. Membr. Sci. 2017, 527, 68-77.

- (28) Wang, Z.; Jin, J.; Hou, D.; Lin, S. Tailoring surface charge and wetting property for robust oil-fouling mitigation in membrane distillation. J. Membr. Sci. 2016, 516, 113-122.
- (29) Yang, J.; Song, H.; Yan, X.; Tang, H.; Li, C. Superhydrophilic and superoleophobic chitosan-based nanocomposite coatings for oil/ water separation. Cellulose 2014, 21 (3), 1851-1857.
- (30) Kota, A. K.; Kwon, G.; Tuteja, A. The design and applications of superomniphobic surfaces. NPG Asia Mater. 2014, 6 (7), e109.
- (31) Liu, T. L.; Kim, C.-J. C. Turning a Surface Superrepellent Even to Completely Wetting Liquids. Science (Washington, DC, U. S.) 2014, 346 (6213), 1096-1100.
- (32) Tuteja, A.; Choi, W.; Ma, M.; Mabry, J. M.; Mazzella, S. a; Rutledge, G. C.; McKinley, G. H.; Cohen, R. E. Designing superoleophobic surfaces. Science 2007, 318 (5856), 1618-1622.
- (33) Tuteja, A.; Choi, W.; Mabry, J. M.; McKinley, G. H.; Cohen, R. E. Robust omniphobic surfaces. Proc. Natl. Acad. Sci. U. S. A. 2008, 105 (47), 18200-18205.
- (34) Israelachvili, J.; Pashley, R. The hydrophobic interaction is long range, decaying exponentially with distance. Nature 1982, 300, 341-
- (35) Tsao, Y.; Evans, D.; Wennerstrom, H. Long-range attractive force between hydrophobic surfaces observed by atomic force microscopy. Science (Washington, DC, U. S.) 1993, 262 (5133),
- (36) Meyer, E. E.; Rosenberg, K. J.; Israelachvili, J. Recent progress in understanding hydrophobic interactions. Proc. Natl. Acad. Sci. U. S. A. 2006, 103 (43), 15739-15746.
- (37) Chen, S.; Li, L.; Zhao, C.; Zheng, J. Surface hydration: Principles and applications toward low-fouling/nonfouling biomaterials. Polymer 2010, 51 (23), 5283-5293.
- (38) Israelachvili, J. Intermolecular and Surface Forces, 3rd ed.; Elsevier: Amsterdam, 2010.
- (39) Tiraferri, A.; Kang, Y.; Giannelis, E. P.; Elimelech, M. Superhydrophilic thin-film composite forward osmosis membranes for organic fouling control: Fouling behavior and antifouling mechanisms. Environ. Sci. Technol. 2012, 46, 11135-11144.
- (40) Lu, D.; Cheng, W.; Zhang, T.; Lu, X.; Liu, Q.; Jiang, J.; Ma, J. Hydrophilic Fe2O3 dynamic membrane mitigating fouling of support ceramic membrane in ultrafiltration of oil/water emulsion. Sep. Purif. Technol. 2016, 165, 1-9.
- (41) Rinaudo, M. Chitin and chitosan: Properties and applications. Prog. Polym. Sci. 2006, 31 (7), 603-632.
- (42) Howarter, J. a; Youngblood, J. P. Amphiphile grafted membranes for the separation of oil-in-water dispersions. J. Colloid Interface Sci. 2009, 329 (1), 127-132.
- (43) Anjali Devi, D.; Smitha, B.; Sridhar, S.; Aminabhavi, T. M. Pervaporation separation of isopropanol/water mixtures through crosslinked chitosan membranes. J. Membr. Sci. 2005, 262 (1-2),
- (44) Dudchenko, A. V.; Rolf, J.; Shi, L.; Olivas, L.; Duan, W.; Jassby, D. Coupling Underwater Superoleophobic Membranes with Magnetic Pickering Emulsions for Fouling-Free Separation of Crude Oil/Water Mixtures: An Experimental and Theoretical Study. ACS Nano 2015, 9 (10), 9930-9941.
- (45) Huang, Y.-X.; Wang, Z.; Hou, D.; Lin, S. Coaxially Electrospun Super-amphiphobic Silica-based Membrane for Anti-surfactant-wetting Membrane Distillation. J. Membr. Sci. 2017, 531, 122-128.
- (46) Zhu, X.; Dudchenko, A.; Gu, X.; Jassby, D. Surfactant-stabilized oil separation from water using ultrafiltration and nanofiltration. J. Membr. Sci. 2017, 529, 159-169.